DEVELOPMENT AND MODELING OF A

SOLAR POWERED GROUND SOURCE HEAT PUMP SYSTEM

by

DEFENG QIAN

ZHENG O'NEILL, COMMITTEE CHAIR
KEITH WOODBURY
SHUHUI LI

A THESIS

Submitted in partial fulfillment of the requirements
for the degree of Master of Science
in the Department of Mechanical Engineering
in the Graduate School of
The University of Alabama

TUSCALOOSA, ALABAMA

2017

ABSTRACT

Buildings consumed 40% of the energy and represented 40% of the carbon emissions in the United States. This is more than any other sector of the U.S. economy, including transportation and industry. Most building energy consumption is for space heating, cooling and water heating in buildings. Enhancing building efficiency represents one of the easiest, most immediate and most cost-effective ways to reduce carbon emissions. One of energy efficient and environment friendly technologies with potentials for savings is Ground Source Heat Pump (GSHP) system. On the other hand, solar energy is considered as an unlimited an environment friendly energy source, which has been widely used for solar thermal and solar power applications.

This study presents a laboratory test facility for a solar powered ground source heat pump system. The ultimate technical goal is to apply the solar powered ground source heat pump into a net-zero energy building (NZEB), where all the electricity consumption will be covered by an integrated on-site solar Photovoltaics (PV) panels and battery system. In addition, an equation based object-oriented modeling language, i.e., Modelica [1] is being investigated for the integrated system modeling. Such dynamic model will be used to explore advanced control of a solar powered GSHP system to facilitate better building to grid integrations.

The detail for the design and layout of this solar powered GSHP system, together with the monitoring and data acquisition system and its Modelica-based dynamic model are introduced in this thesis. In addition, the feasibility of the application of the system are discussed. Finally yet importantly, the future work are presented.

LIST OF ABBREVIATIONS AND SYMBOLS

CMHC	Canada Mortgage and Housing Corporation
COP	Coefficient of Performance
DX	Direct Expansion
EU	European Union
HVAC	Heating, Ventilation and Air-Conditioning
GCC	Global Climate Change
GHG	Greenhouse Gas
GHI	Global Horizontal Irradiation
GSHP	Ground Source Heat Pump
GUI	Graphic Use Interface
NZEB	Net-zero Energy Building
SOC	State of Charge

ACKNOWLEDGMENTS

I would first like to thank my thesis advisor Dr. Zheng O'Neill at Department of Mechanical Engineering in the University of Alabama. The door of Dr. O'Neill's office was always open whenever I have questions about my research or writing. She consistently offer me the freedom to explore my own ideas, but steered me in the right direction.

I would also like to thank my thesis committee members, Dr. Keith Woodbury and Dr. Shuhui Li. I appreciate their committed service, supports, ideas, and valuable comments on the thesis improvement.

My appreciation also extends to my colleagues at the University of Alabama High Performance Building Laboratory, both present and former, namely, Fuxin Niu, Yanfei Li, Zhengwen Hao, Liu Liu and Zilai Zhao for their supports and help in direct or indirect ways.

Finally, I must express my very profound gratitude to my parents for providing me with unfailing support and continuous encouragement throughout my years of study and through the process of researching and writing this thesis.

The accomplishment would not have been possible without the support and effort from them. Thank you.

CONTENTS

LIST OF TABLES

LIST OF FIGURES

1. INTRODUCTION

According to the recent research [2], from 2007 to 2035, the global demand for oil will increase by 30%, while the demand for coal and natural gas will increase by 50%. Those data informs us that energy-related carbon emissions will increase significantly if there are no radical changes of the energy structure [3]. Meanwhile, the U.S. consumed 17% of the energy in the world, while buildings consumed 40% of the energy and represented 40% of the carbon emissions in the U.S. [4]. This is more than any other sectors of the U.S. economy, including transportation and industry. About 24% of all energy used in the nation was for space heating, cooling and water heating in the buildings [4]. Improving energy efficiency and reducing energy consumption in buildings is one of the most important priorities during the operation stages of buildings.

Enhancing building efficiency is one of the simplest, most immediate and most cost-effective ways to reduce the carbon emissions. In addition, integrating renewable energy sources into an efficient Heating, Ventilation and Air-Conditioning (HVAC) would make a net-zero energy building (NZEB) become possible. Theoretically, the goal of NZEB is to reduce the energy consumption (and demand) through efficient designs and operations, and utilize the renewable energy as a major energy source while the conventional energy sources play a backup role in the buildings. The key points of the goal of NZEB include: 1) a high efficient building envelope, 2) high performance HVAC system with advance control strategy, and 3) on site renewable energy source.

As one of the most efficient system the market, the GSHP is considered as one of the best solutions for the building HVAC system for a wide variety of geology conditions. The GSHP utilizes the relatively constant temperature of the ground, ground water, and surface water, and it is about 45% more efficient than conventional heat pumps [3].

On the other hand, renewable energy is defined as a kind of energy can be replenished with the passage of time [3]. Solar energy is one type of renewable energy, which can be considered as an unlimited an environment friendly energy source, which has been widely used for solar thermal and solar power applications.

In general, high-performance system could be less efficient without the appropriated and robust control strategies. Model-based control has been widely used in automobile, aerospace and industry process, and starts to be emerged in building industry. In this study, a Modelica-based dynamic model is developed to help understand the dynamics of solar powered GSHP system. As a hierarchical object-oriented physical modeling language, the models in Modelica are mathematically described by differential, algebraic and discrete equations [5].

This thesis is organized as follows: Chapter Two is the literature review for the related work, which covers Net-Zero Energy Building (NZEB), Ground Source Heat Pump (GSHP), Renewable Energy, and Modeling with Modelica. Chapter Three is Method and Approach. The GSHP and solar panel equipment, GSHP system setup, and the analysis methodology will be introduced in Chapter Three, followed by results and discussions in Chapter Four. Finally, yet importantly, the future work will be introduced in Chapter Five.

This thesis covers the preliminary on-site measurements from a test rig of a solar powered ground source heat pump system and initial simulated results from a Modelica model. The on-site measurements include the theoretical estimation and actual measurements of the

solar power generation, energy consumption of the system, the cooling rate of the heat pump, and coefficient of performance (COP) of the heat pump and the system. Since the Modelica model for the test rig is still under development, no validations of the system model with measurements are included.

2. LITERATURE BACKGROUND REVIEW

2.1 Net-Zero Energy Building (NZEB)

Energy consumption in building is very important considering its large share of the U.S. total energy consumption. To counteract the global climate change (GCC) trend, the concept of "Net-Zero Energy Buildings" (NZEB) is being studied and to small extent already implemented in the field to reduce the building energy consumption and the use of fossil fuels, which is the most important contributor to GCC [6]. The word "Equilibrium Sustainable House" was used by Canada Mortgage and Housing Corporation (CMHC) instead of "Net-Zero Energy Buildings" for those houses that are actually on-grid NZEB. This type of building is connected to one or more energy infrastructures such as electricity grid, district heating and cooling system, gas pipe network, and biomass and biofuels distribution networks [6]. On the other hand, there is another type of NZEB called off-grid NZEB, which is not connected to a utility grid and hence needs an energy storage system such as batteries or thermal storage, does not get much attention from the government, industry or academic because most of the buildings are not isolated and often located in an environment where other buildings exist [6]. This study is focusing on the second type of NZEB, which is off-grid NZEB.

2.2 Ground Source Heat Pump (GSHP)

The world has started facing some local and global problems caused by the utilization of unsustainable energy sources. One of the most significant problems is global warming, as a result

of drastically increased greenhouse gas (GHG) emission [7]. GSHP system combines the heat pump and a ground loop heat exchanger for transferring the heat between the GSHP system and the ground source. This type of system has been in use for years due to its outstanding efficiency compared to those conventional heating and cooling equipment. For those conventional cooling and heating equipment such as air-source heat pumps, outside temperature would cause a significant impact on its efficiency. On the other hand, GSHP system overcomes the problem of resource variation, as ground temperature remain fairly constant throughout the year. Refer to Ozgener and Hepbasli [8, 9], GSHPs have following advantages:

- They consume less energy to operate
- They tap the earth or groundwater, a more stable energy source than the air
- They do not require supplemental heat during extreme low outside temperature
- They use less refrigerant
- They have a simpler design and consequently less maintenance, and
- They do not require the unit to be located where it is exposed to weathering.

There are three types of GSHP system, open-loop system, closed-loop system, and semi-open-loop system. According to Huttrer [10], open-loop systems are simple: water is pumped out of a well, a surface water body or even a municipal water system component, passed through the heat pump heat exchanger and then discharged back into the source . Open-loop system is most inexpensive and efficient; however, their use can lead to a need for frequent maintenance, such as cleaning of the heat exchanger, addition of chemical inhibitors to prevent fouling of loops by organic matter and etc. For the closed-loop systems, water or a water-antifreeze solution circulates in a continuous buried pipe, while a heat exchanger helps transfer the energy between the ground source and circulated water. The semi-open-loop system (i.e., standing column well

system) combines the advantage of both open-loop system and close-loop system. Figure 2-1 shows schematics of different ground source heat pump system. The experiment and dynamic model in this study are based on an open GSHP system as shown in Figure 2-2.

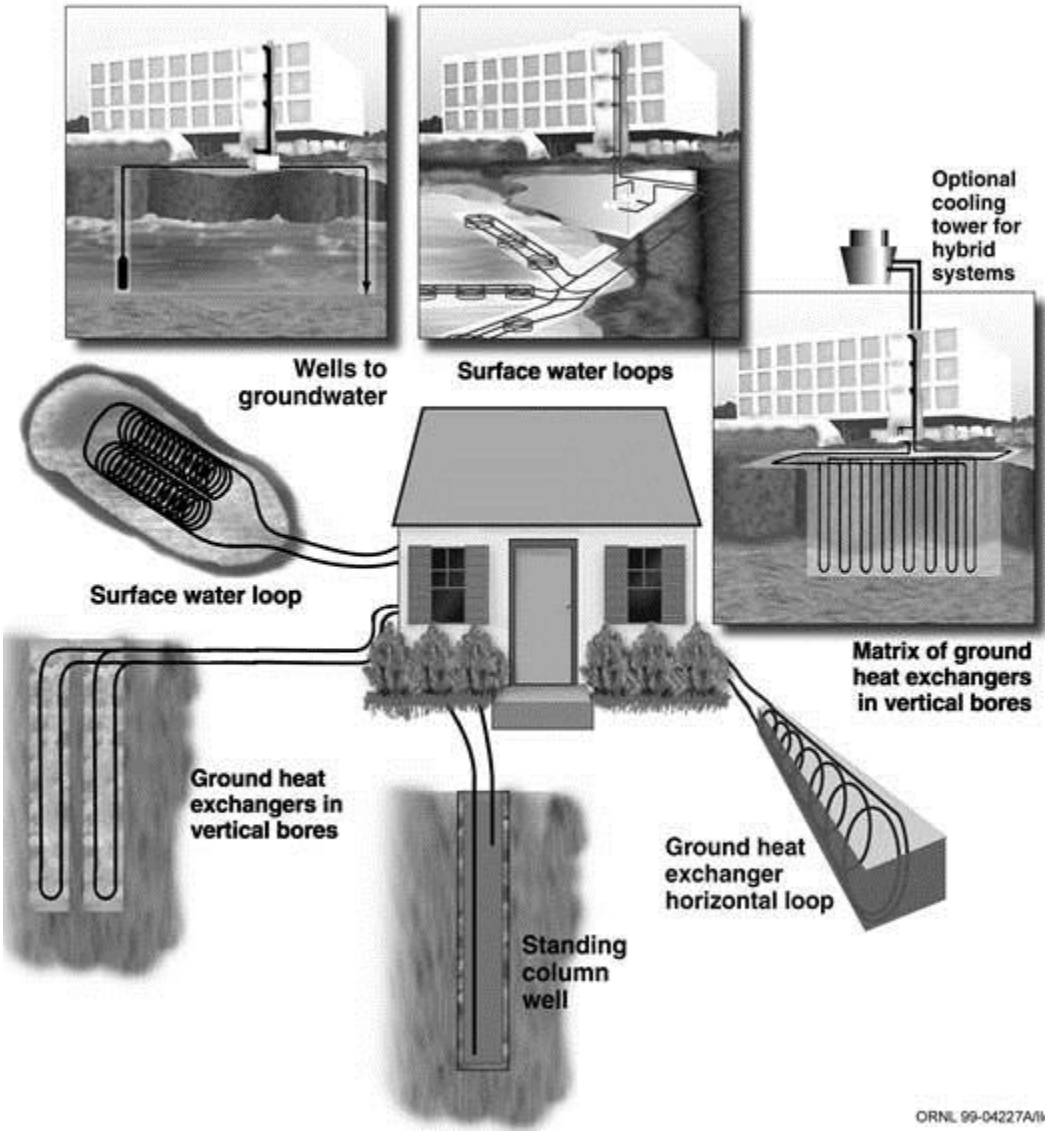

Figure 2-1 Schematics of Different GSHP Systems.

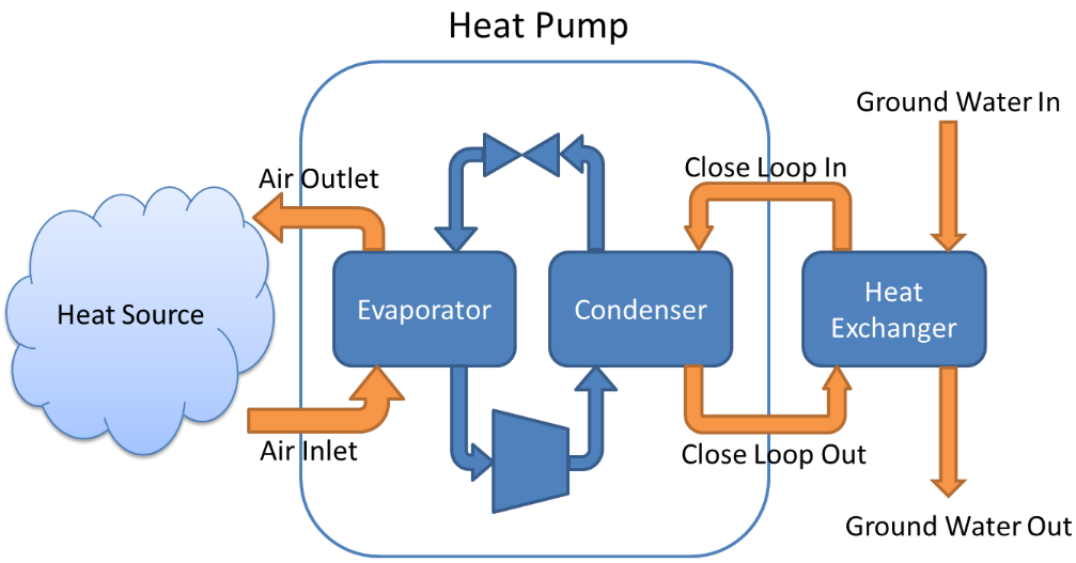

Figure 2-2 An Open GSHP System for This Study.

According to Self's research [11], GSHP system is able to work with soil and ground water temperature between 5˚C and 30˚C (41˚F to 86˚F). The GSHP system has been commonly used in 30 countries since 2004. United States, Sweden, German, Switzerland, Canada, and Austria are the leading countries in the group. The annual growth rate of GSHP is about 10% since 1994, and there were approximately 1.7 million applications in 2012.

According to Zhu, Tao and Rayegan [12], there would be about seven to eight percent energy savings using the GSHP system compared with the conventional system. Studies have proved the performance of the GSHP system from an economic perspective. GSHP system shows its advantages in those studies in terms of the life cycle cost and the payback period. For example, Shonder [13] conducted a study of life cycle cost for GSHP system, and the result shows GSHP system is the most cost-effective options among the others. Another study from Chiasson [14] shown the similar result that GSHP system has the lowest life cycle cost compared to the rooftop units with gas heating and direct expansion (DX) cooling and air-source

heat pump.Although Zhu, Tao and Rayegan [12] mentioned a 12 to 15 years' payback period, which is a relatively long payback time considering the external factors such as reliability, climate change, and etc., reduction of initial installation cost for the GSHP system could shorten the payback period significantly.

Self's study [11] also included a comparison of carbon dioxide (CO_2) emission between different HVAC systems. Although the HVAC system usually does not emit CO_2 directly, its energy consumption is strongly correlated with CO_2 emissions. Since power plants generating electricity usually produce high CO_2 emissions, the utilization of high performance HVAC system such GSHP system greatly reduce the CO_2 emission and mitigate the greenhouse effect.

2.3 Renewable Energy (Solar Energy)

With the growing population and technology evolutions, the demand of energy source increased significantly in past decades. According to a study from Kannan, world total energy consumption reached 520 Quadrillion Btu in year 2011 [15] . Figure 2-3 shows the tendency of the world population since year 1980, and Figure 2-4 shows tendency of primary energy consumption in the world.

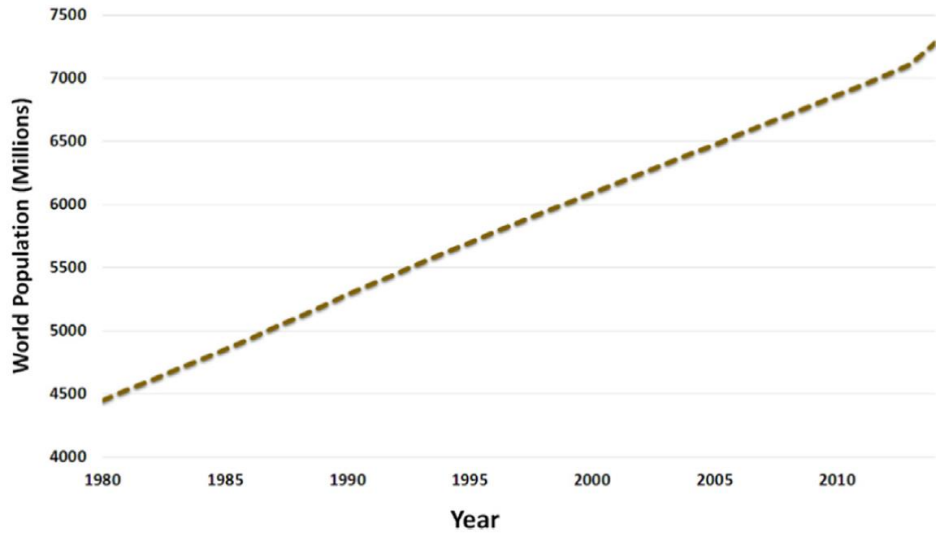

Figure 2-3 World Population Status [15].

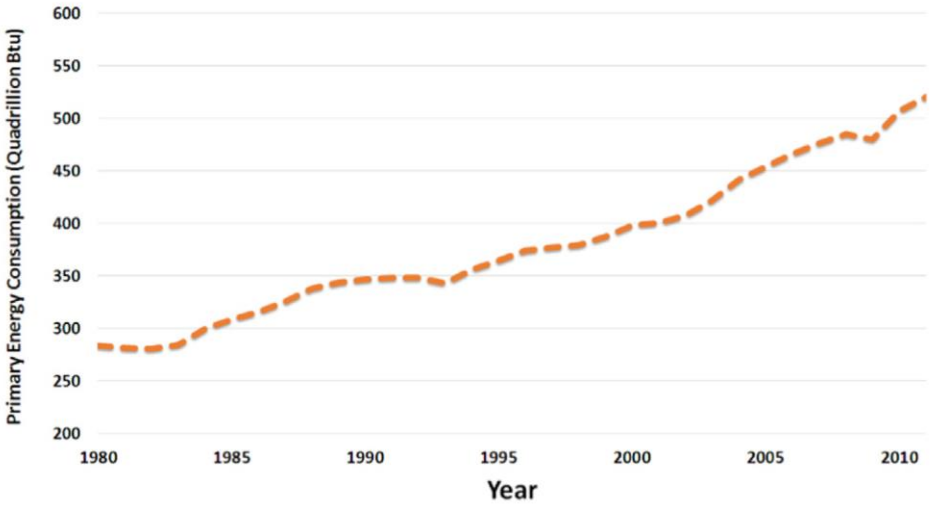

Figure 2-4 Total Primary Energy Consumption [15].

Currently, the primary source of the energy generation is fossil fuels, which are finite resource and responsible for significant carbon emissions. People already saw the shortage of fossil fuels with increasing demand of energy. This type of situation motivates people to explore an alternative way to satisfy the energy demand [11]. Meanwhile, emission of CO_2 from burning

the fossil fuel is affecting the environment. Tripathy's study [16] predicts the total emission of CO_2 will exceed 10 billion tons by the end of year 2030. According to the current situation, it is urgent to find the replacement of the current primary source. The alternative source should have following benefits:

- Low carbon emissions and environmental friendly
- Low maintenance and operation cost
- High usability
- High efficiency

By combining these benefits, renewable energy sources become an optimal alternative solution for increasing demand of energy. There is a trend that more and more people began to accept the renewable source. For example, the European Union (EU) set a target that the renewable energy will contribute 20% of the energy by the year 2020, and the number will increased to 27% by the year 2030 [17].

Renewable energy is a generalized definition for the clean energy; it can be divided into several main sectors, such as hydropower, wind power, bio power, solar PV, geothermal etc. Kannan's research [15] indicates in 22.1% of total electricity production in year 2013 is from renewable source, among which, 16.4% is from hydropower, 2.9% is from wind power, and only 0.7% of the energy is from solar PV. Figure 2-5 shows a pie chart of global electricity production in year 2013. The study indicates a huge potential for the solar PV industry to play a more important role in the future.

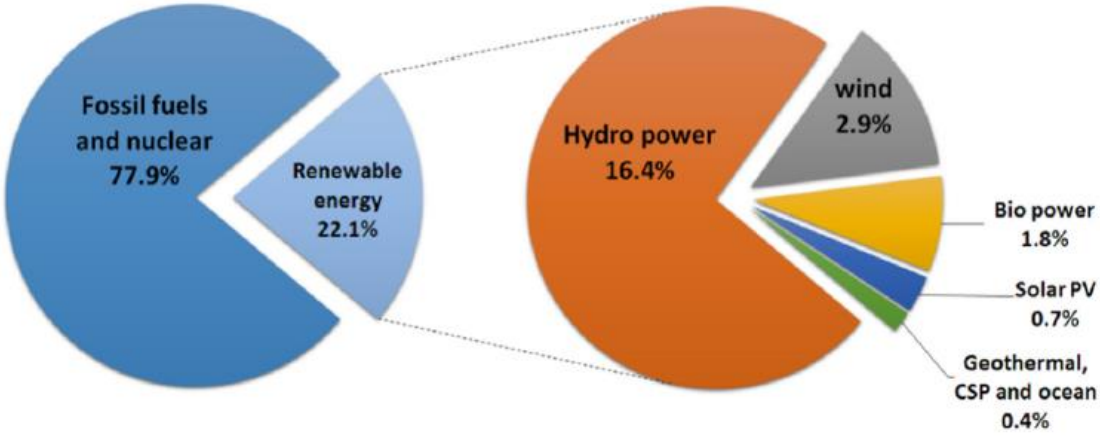

Figure 2-5 Global Electricity Production in Year 2013 [15].

Solar energy is not only a promising source, but also an abundant energy. Fig. 2-6 shows a map of global horizontal irradiation (GHI). The map shows the potential solar energy is at a range of 1500 to 2200 kWh/m^2 in the United States [15]

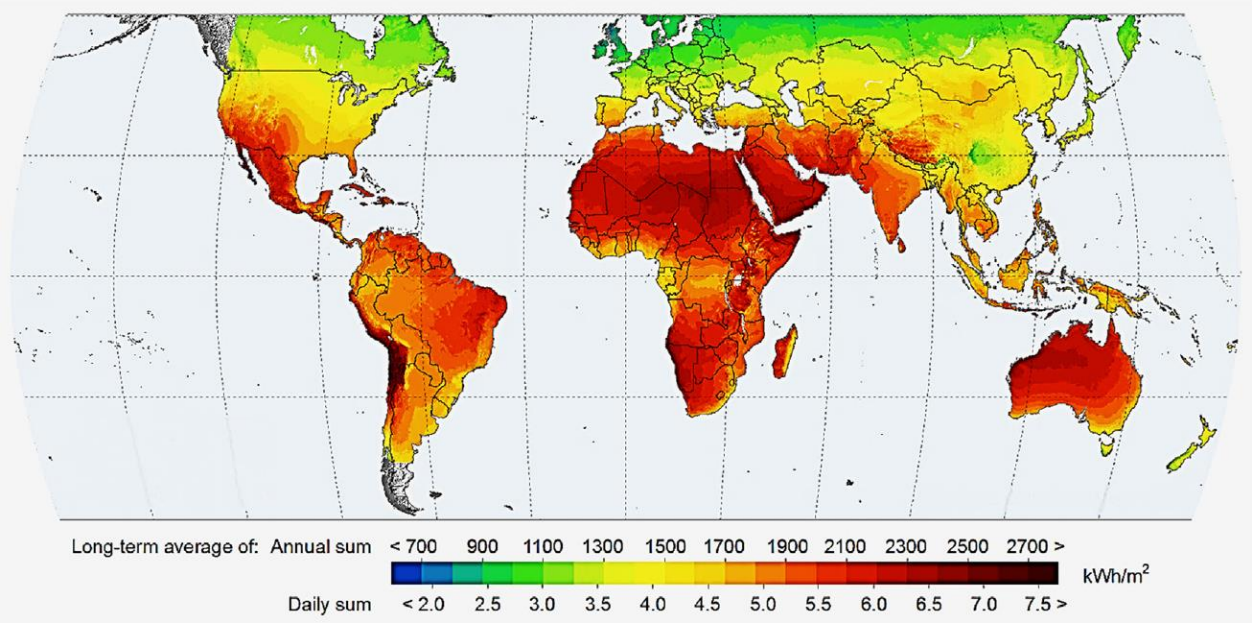

Figure 2-6 Maps of Global Horizontal Irradiation (GHI) [15].

Kannan's study [15] shows solar electricity generation increased significantly after year 2007. Figure 2-7 shows the solar electricity net generation from year 1980 to 2010 in Billion Kilowatt-Hour (kWh). In addition, solar PV has the largest annual growth rate in year 2013 (Figure 2-8). Nowadays, solar PV technology is widely used in different area, such as building HVAC system, industrial heat generation, water heating, even cooking and drying.

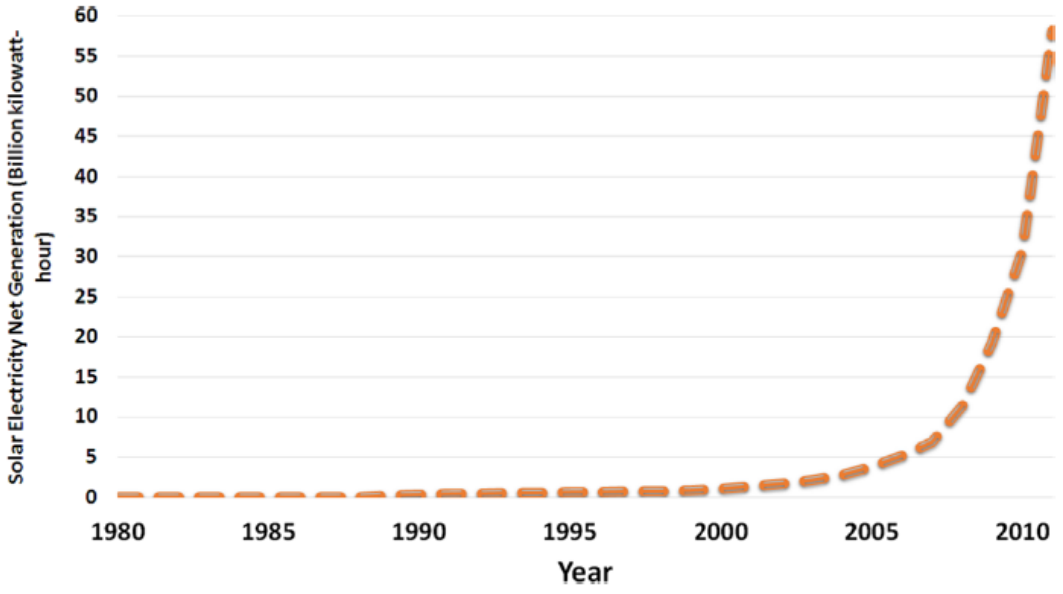

Figure 2-7 Solar Electricity Net Generation (in Billion kWh) [15].

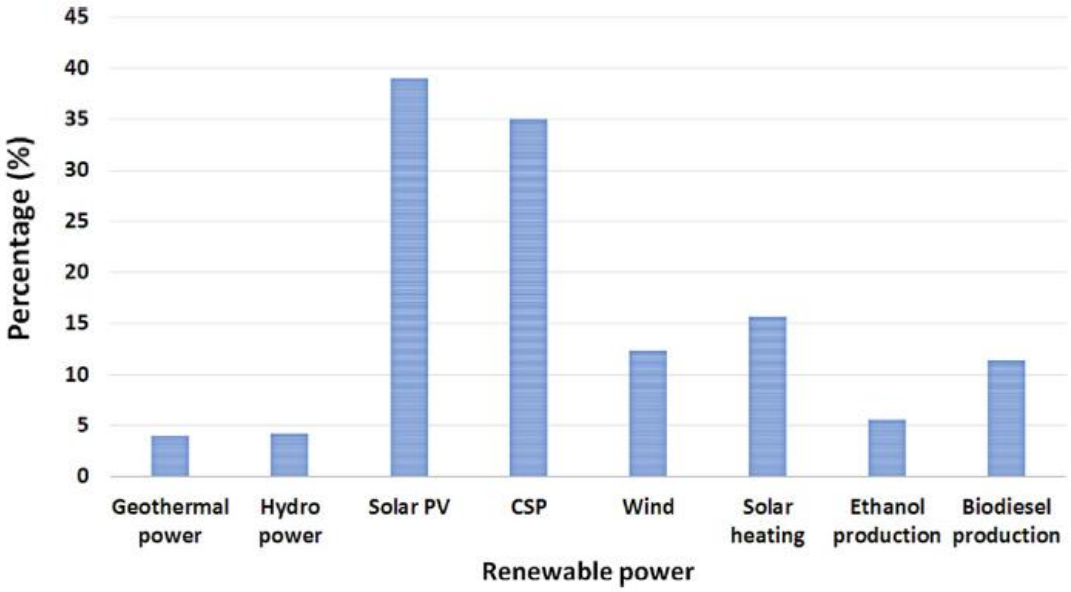

Figure 2-8 Annual Growth Rate of Renewable Energy Capacity in 2013 [15].

2.4 Modeling with Modelica

As the mathematical modeling and simulation became the key factors in engineering, computerized tools were developed to satisfy the needs of efficient engineering. As the needs of simulation tools increases, people realized most simulation tools were developed for their corresponding purpose, which limits the usability between different studies of area. According to Mattsson's study [18], although there are many simulation software on the market, most languages and model representations are proprietary. Most simulation software are focusing on one domain, which with no capability in other field of area.

A new language, called Modelica was developed, which has the capability to switch the models between libraries easily. Modelica is a hierarchical object-oriented, non-proprietary, equation based language, which can be easily used to model complex physical system, e.g., mechanical, electrical, electronic, hydraulic, thermal, control, electric power or process-oriented

subcomponents [1]. According to Mortada's study [19], Modelica is a modeling language, not a programming language. It supports library components, connects, and composite acausal connections. In addition, Mattson's study [18] also pointed, "Algorithms and functions are supported in Modelica for modeling parts of a system in procedural programming style. Constructs for including graphical annotations are available, in order that icons and model diagrams also become portable. An extensive Modelica base library contains standard variable and connector types to promote reuse by standardizing on interfaces".

Generally, the ideal scenario for the modeling is that users should have a finished model for their special purpose, which can be defined as the low level, such as equations and basic phenomenal. Meanwhile, an optimal condition is that users can develop models based on different libraries depends on their needs. The second scenario is often referred as modeling with higher hierarchical levels, and Modelica language is aiming to achieve such structure.

Overall, the most important reasons to adopt Modelica for modeling are as follows:

- Instead of assignment statements, Modelica is based on equations.
- Modelica has the capability to simulate under multi-domain condition.
- Modelica is an object-oriented language which can be re-used in different group assembly.

The model used in this study is developed using the Modelica language and it uses the commercial simulation environment and system solver Dymola [20] . In this study, a commercial Modelica library - Vapor Cycle Library is adopted for the steady-state and transient simulation of a refrigeration cycle in heat pump. Vapor Cycle Library is a commercial and licensed Modelica library typical vapor compressor cycle applications. The Vapor Cycle Library contains component and system models for refrigeration processes including air-conditioning

applications, heat pumps, organic Rankine Cycle, etc. The Vapor Cycle Library is compatible with other Modelica libraries such as Liquid Cooling Library, Heat Exchanger Library and other Modelica mechanical and electrical libraries [21]. The features of the Vapor Cycle Library includes [21]:

- Comprehensive set of vapor cycle components that reduce the modeling time.
- Transient and steady-state modes that enables users to simulate real-world behavior early in the design process.
- Wide range of working fluids, including R134a, R774 and R1234yf.
- Based on the Modelica Language open standard, enabling model re-use and easy integration with other libraries.

Dymola has a relative user-friendly interface. The component parameter dialogs are structured using tabs and grouping, with text and graphical explanations [22]. Figure 2-9 shows a sample parameter inputs graphic use interface (GUI) of an Evaporator.

In this study, a dynamic model is created with existing components from the Vapor Cycle Library and ThermoFluidPro Library from Modelon [21]. In the near future, this model will be validated using the data collected from the solar powered GSHP system test rig.

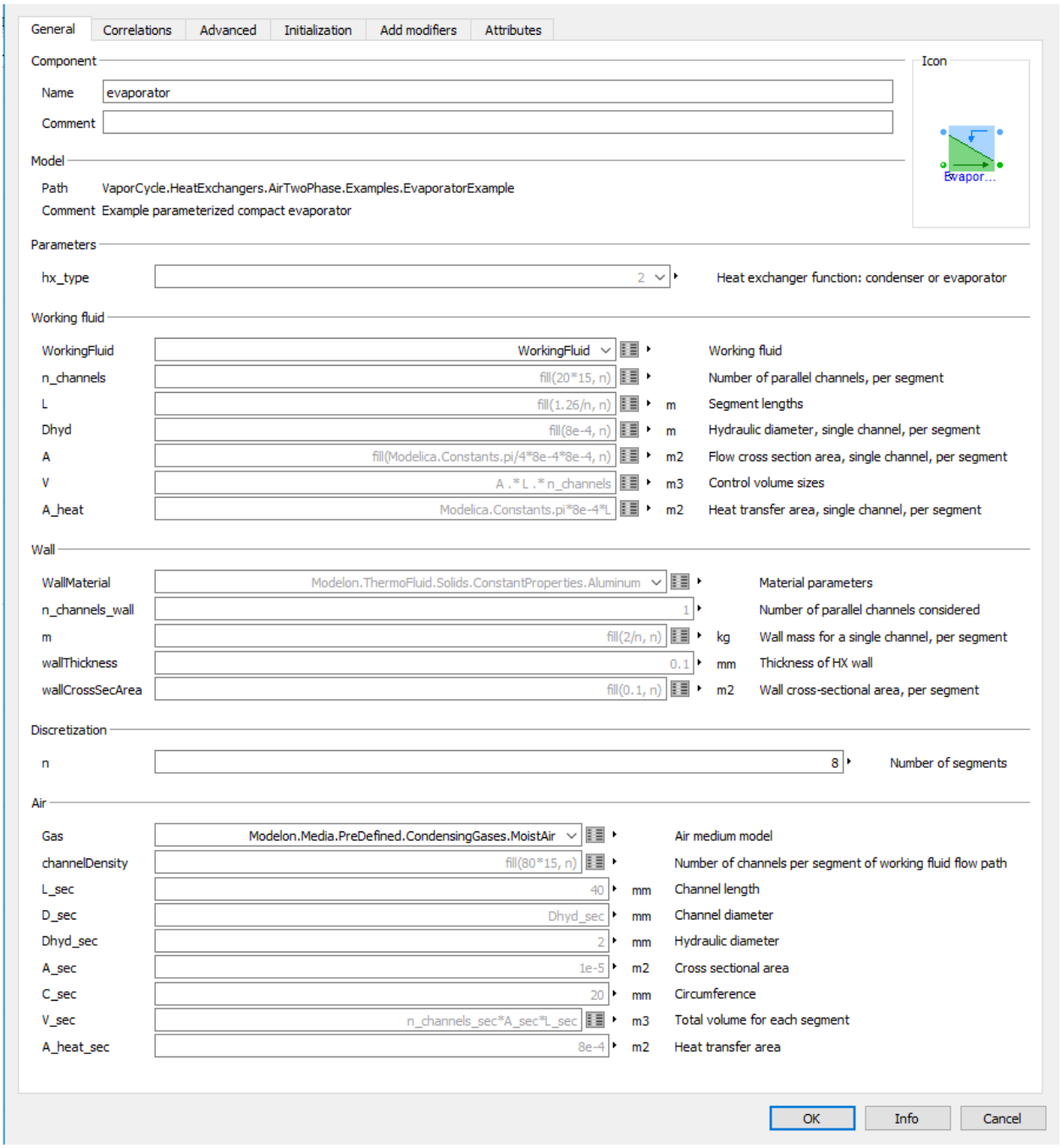

Figure 2-9 A Sample Parameter Dialog of an Evaporator.

3. METHOD AND APPROACH

3.1 System Description

In this study, a solar powered GSHP system is built for test purpose. In this test fig, a ¾-ton water-to-air GSHP is connected to two 60-feet deep walls (Figure 3-1 Design and setup). A group of Solar PV panels of 1.12 kW is connected to two 800 Ah battery banks, which are used to power the GSHP system and a 270 Watts DC powered well pump. During the daytime, solar PV panels convert solar photons into electrical energy, which will be stored into battery banks. Whenever the system is on demand, the battery banks can provide the electricity power.

Due to the low pH of the groundwater while the water quality at this site is good, a heat exchanger is introduced between the heat pump condenser and the ground water loop. Figure 3-2 depicts the GSHP system with accessories including a circulation water pump, various sensors, a heat exchanger, etc.

In addition, a comprehensive performance monitoring and data acquisition system is installed. Table 3-1 lists the major sensors deployed in this test rig.

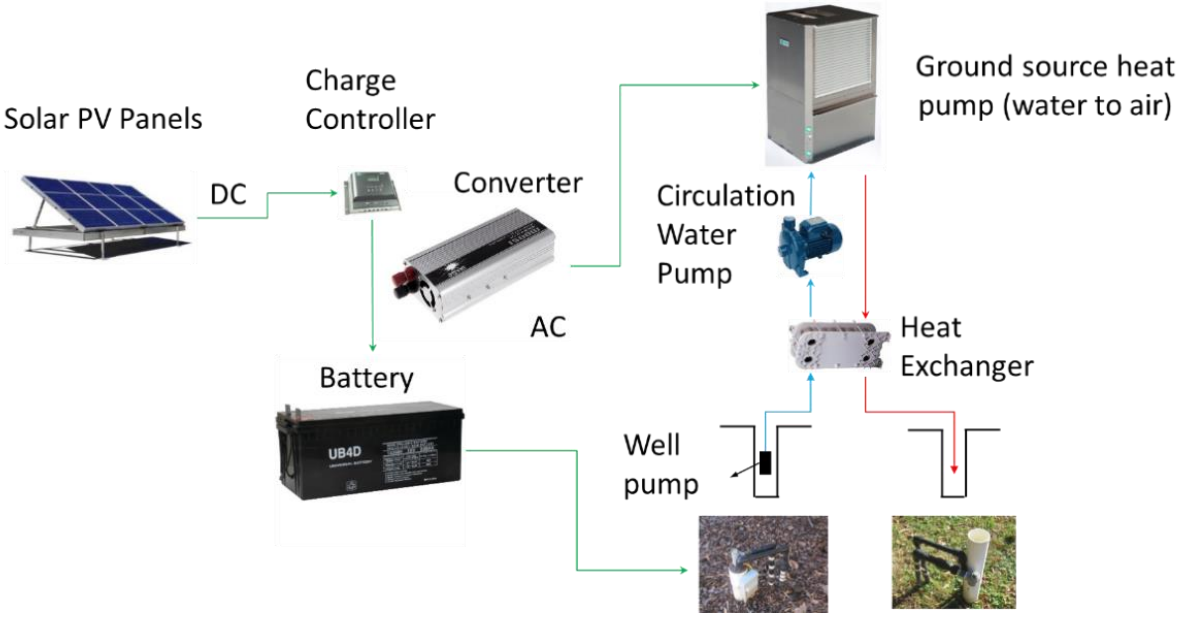

Figure 3-1 System Design and Setup.

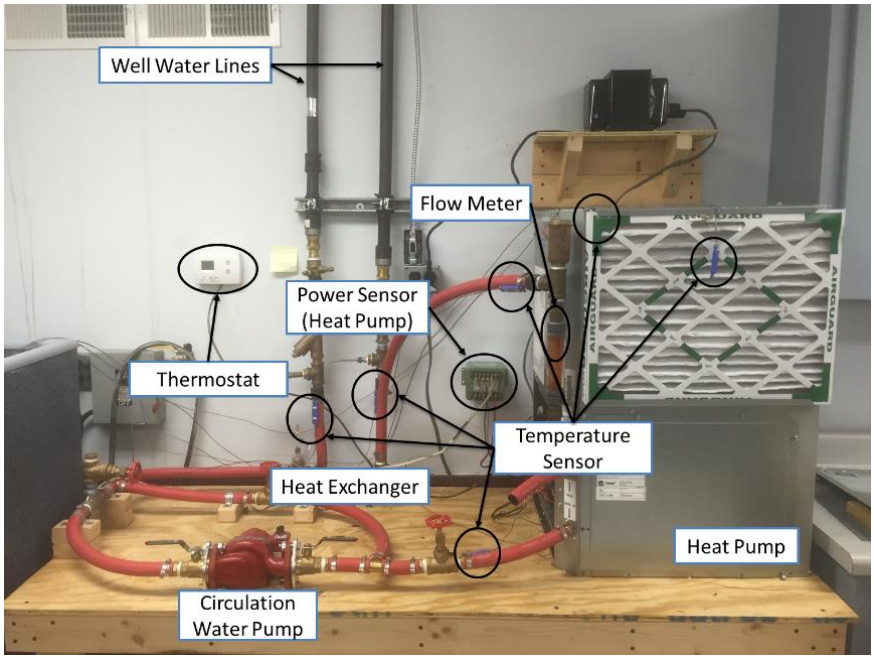

Figure 3-2 the Setup of GSHP in the Lab.

Table 3-1 Major Sensors Deployed in the Test Rig.

Position	Sensor*
Ground Water Inlet (from the well)	Temperature Sensor 1
Ground Water Outlet (to the well)	Temperature Sensor 2
Circulate Water Inlet (to the GSHP)	Temperature Sensor 3
Circulate Water Outlet (from the GSHP)	Temperature Sensor 4
Air Intake (to the GSHP)	Temperature Sensor 5
Air Outlet (from the GSHP)	Temperature Sensor 6
Power Sensor (GSHP)	Power Transducer
Solar Panel Input Voltage	Voltage Divider
Solar Panel Input Current	Current Shunt
Circulation Loop (closed water loop)	Flow Meter

*The temperature sensor is a T-type thermocouple.

3.2 Equipment Description

3.2.1 Heat Pump

The heat pump adopted in this study has a rotary type compressor, rated cooling capacity is 10200 Btu/hr (2989 Watts) and heating capacity is 9300 Btu/hr (2725 Watts). The refrigerant is R-410a, and the charging weight is 26.5 OZ (0.751KG). Under a normal operating condition, the pressure of the refrigerant is 450 psig (3103 kPa) for the high side, and 250 psig (1724kPa) for the low side. On the waterside, the maximum working pressure of the water is 400 psig (2757

kPa). For the airside, the maximum external static is 70 inches water gauge (inWG). In addition, the rated operating voltage is 208 Volt, and short circuit current rating is 5kA at 600V.

3.2.2 Solar Panels

There are two sets of solar panels were used in this study. The first set was installed around 20 years ago, and the second set was installed in year 2015.

The first set of solar panels has 20 panels in two groups, and 16 of them were utilized in this study. Each panel in the first set has a rated power output of 50 Watts. Theoretically, 16 of them will output a maximum of 800 Watts. Table 3-2 shows the electrical parameters of each panel. The nominal operating cell temperature is 45˚C (113˚F), and the sensitivity of the panel is +1.2mA/˚C, -0.071 Volts/˚C. The performance of these solar panels is tested under the certain conditions. Table 3-3 shows the qualification test parameters. From the manufacturing specification, these solar panels are guaranteed for 90% of the minimum power in the first 10 years, and 80% of the minimum power in the first 25 years.

The second set of solar panels has four panels, and all of them were used in this study. Each panel in the second set has a rated power output of 80 Watts, and total maximum output would be 320 Watts. Table 3-4 shows the electrical parameters of each panel. The performance of these solar panels is tested under the certain conditions. Table 3-5 shows the qualification test parameters. From the manufacturing specification, these solar panels are guaranteed for 90% of the minimum power in the first 12 years, and 80% of the minimum power in the first 25 years.

For both two sets of solar panels, the solar panels performances were calibrated at the solar irradiation level of 1000W/m^2. Figure 3-3 shows the actual setup of the solar panels. The first set of the solar panels has a net output for 800 Watts, and the second set of the solar panels has a net output for 320 Watts.

Meanwhile, the orientation of the solar panels is a key factor to maximize the receiving the solar radiations. According to Tripathy's study [16], some models are already existed for the optimal tilt angle at different locations by following analytical and experimental methods. In general, the optimum tilt angle is approximately the same as the latitude of the location.

The test rig is located at Tuscaloosa, and the corresponding latitude is 33.2˚. Therefore, the tilt angle of the solar panel in this study is set at 30˚.

Table 3-2 Electrical Parameters of the First Solar Panels Set.

Maximum Power Rating	[Watts]	50
Minimum Power Rating	[Watts]	45
Rated Current	[Amps]	3.15
Rated Voltage	[Volts]	15.9
Short Circuit Current	[Amps]	3.35
Open Circuit Voltage	[Volts]	19.8

Table 3-3 Qualification Test Parameter of the First Solar Panel Set.

Humidity	[% RH]	85
Wind Loading or Surface Pressure	[N/m^2]	2400
Maximum Distortion	[Degree]	1.2
Hailstone Impact Withstand	[mm @ m/s]	25 @ 23

Table 3-4 Electrical Parameters of the Second Solar Panels Set.

Maximum Power Rating	[Watts]	80
Rated Current	[Amps]	4.5
Rated Voltage	[Volts]	17.9
Short Circuit Current	[Amps]	4.8
Open Circuit Voltage	[Volts]	21.9

Table 3-5 Qualification Test Parameter of the First Solar Panel Set.

Humidity	[% RH]	85
Wind Loading or Surface Pressure	[N/m^2]	2400

Figure 3-3 Setup of the Solar Panels.

3.2.3 Weather Station

An on-site weather station is installed to measure outside air temperature, relative humidity, wind speed and direction, and solar radiation intensity (note: total global horizontal solar flux only). The weather station includes a data logger with a WIFI connection, which is capable to work from -40 to 60˚C. The data logger has 512K bytes local storage, and the logging interval can be specified between 1 second to 18 hours. In this study, the weather data sampling frequency is once every 2 minutes. All weather-related data is being pushed to HOBOlink

website every 10 minutes. There are five standard data inputs available for the sensors, and the maximum number of channels can be extended up to 15 channels.

Table 3-6 shows the function of the sensors and their corresponding measurement range and accuracy. Figure 3-4 shows the on-site weather station.

Table 3-6 Specification of Weather Station Sensors.

	Measurement Range	Accuracy
Temperature Sensor	-40 to 75 ˚C	± 0.21 ˚C from 0 to 50 ˚C
Relative Humidity Sensor	10% to 90%	0.1%
Wind Speed Smart Sensor	0 to 76 m/s	± 1.1 m/s or 4% of reading whichever is greater
Wind Direction Smart Sensor	0 to 355 degrees, 5 degree dead band	± 5 degrees
Solar Radiation Smart Sensor	0 to 1280 W/m2	± 10W/m2 or +5%, whichever is greater in sunlight

Figure 3-4 On-Site Weather Station.

3.2.4 Data Acquisition System

The data acquisition is combined with a chassis system, which has 5 hybrid slot, 3 PXI Express lots (up to 250MB/s per-slot bandwidth and 1.75GB/s system bandwidth) and two input modules. The thermocouple input module has 32 channel, 8 built-in cold junction comprehensives channels and 0.3˚C accuracy. The voltage module has 16 analogy inputs, 2 analog outputs, 16-bit resolution and a range of ±10V. The sampling rate is once per second for both temperature and solar power generation. To match the sampling rate of the weather station (once per two minutes), the average of the solar radiation flux over two minutes will be used for the analysis. Figure 3-5 shows the comprehensive data acquisition system that is used for this study.

By using the data acquisition system, well ground water temperatures, refrigerant temperature, air temperature, solar power generation, etc. are all real-time monitored, trended and stored in a database for further analysis.

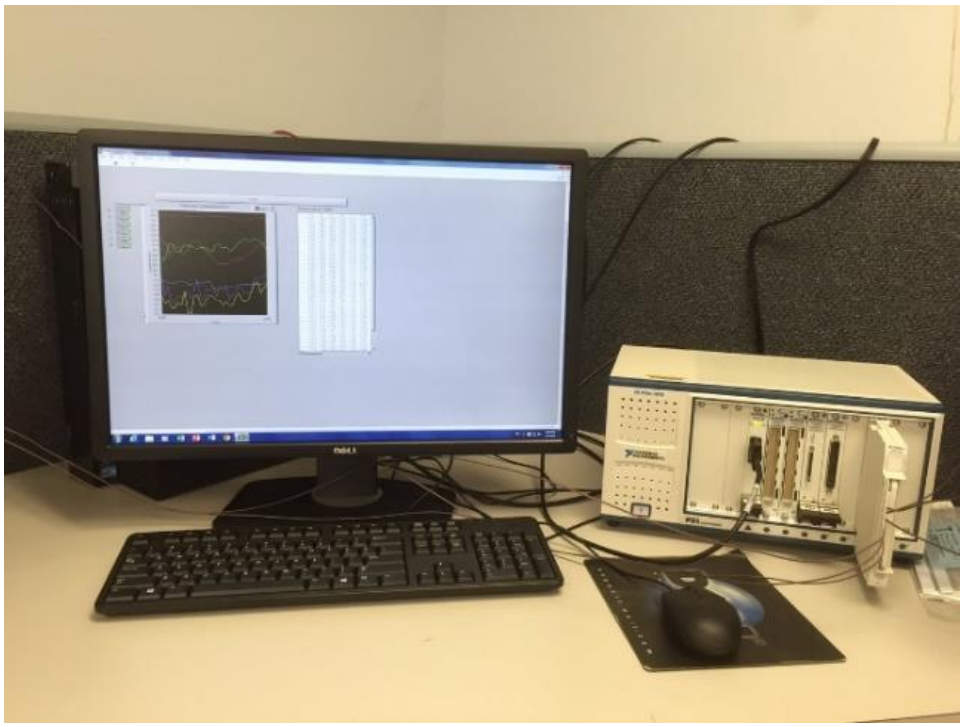

Figure 3-5 Data Acquisition System.

3.2.5 Solar Energy Collection/Power Generation

On the supply side, solar panels will only be able to generate the electric energy during the daytime, which means the batter banks need to store enough for potential demand after the sunset and bad weather such as rainy or cloudy days. The way to monitor the solar energy collection/power generation is this study is to measure the power voltage generated by the solar panels and current flow between the solar panels and the battery banks. Based on the measured voltage and current, the power generation can be calculated based on the following equation:

$$P = V \times I \tag{1}$$

where

P is the power generation from the solar panels (W),

V is the voltage of the solar panels (V),

I is the current flow between the solar panels and the battery bank (A).

Some of solar panels that are connected to the heat pump were installed about 20 years ago, therefore, it is expected that there are some performance degradations. In addition, the solar angle changes through the years. This will cause the fluctuation of electricity energy generation from the solar panels. The following assumptions are used to simplify the calculation:

1) solar energy collection/power generation can be maintained at the peak,
2) the variations of weather impact are neglected,
3) the batteries can continuously store energy from the solar panels,
4) although the manufacture specifies the efficiency of the inverter is up to 93%, an 85% efficiency will be taken during the calculation, and
5) the discharge capacity is at a 70% level of the total capacity of the batteries.

For the charge and discharge time, the following equations are used respectively:

$$t_{charge} = \frac{C_{battery} \times V_{battery}}{P_{charge}} \tag{2}$$

where

t_{charge} is the time to charge the battery (hr),

$C_{battery}$ is the capacity of the batteries (Ah),

$V_{battery}$ is the battery voltage (V),

P_{charge} is the charge rate (W).

$$t_{discharge} = \frac{C_{discharge} \times \eta \times V_{battery}}{P_{discharge}} \tag{3}$$

where

$t_{discharge}$ is the time to discharge the battery (hr),

$C_{discharge}$ is the discharge capacity of the battery (Ah),

η is the inverter efficiency,

$P_{discharge}$ is the discharge rate (W).

In general, the battery cannot be fully discharged. Usually, the discharge capacity is about 70% to 80% of the capacity of the battery. In this study, a 70% level of the battery capacity is assumed to be used.

3.2.6 Geothermal Energy Balance

The energy balance between the ground water and the closed-loop water is tested using the following equation:

$$\dot{m}_{GW} \times C_{p_{water}} \times \Delta T_{GW} = \dot{m}_{CL} \times C_{p_{water}} \times \Delta T_{CL} \tag{4}$$

where

$\dot{m}_{GW}$ is the mass flow rate of ground water ($\frac{kg}{s}$),

$\dot{m}_{CL}$ is the mass flow rate of closed-loop water ($\frac{kg}{s}$),

$C_{p_{water}}$ is the specific heat of water ($\frac{J}{kg*K}$),

ΔT_{GW} is the temperature difference between the ground water inlet and outlet (K),

ΔT_{CL} is the temperature difference between the water inlet and outlet of the heat pump (K).

3.2.7 Heat Pump Energy Balance

The total energy balance represents the system performance in either the cooling or the heating mode. The total energy balance is based on the energy consumption of the heat pump, the heat exchange rate between the waterside and airside of the heat pump, and the cooling or heating rate of the heat pump. In this paper, all the tests are conducted for the cooling mode. The following equation is used to calculate the cooling rate and check the total energy balance.

$$P_{heat\ pump} + q_{rej} + q_{cooling} = 0 \tag{5}$$

where

$P_{heat\ pump}$ is the power input of the heat pump (W),

q_{rej} is the heat rate rejected to the water-side of the heat pump (W),

$q_{cooling}$ is the cooling rate of the heat pump (W).

The energy consumption of the heat pump is monitored by the data acquisition system and energy exchanged between the waterside and the airside will be calculated using the measured data including temperatures and flow rates. The actual cooling rate will be calculated using Equation (5).

3.2.8 The Coefficient of Performance (COP)

The COP is a dimensionless parameter which is used to measure the efficiency of the heat pump. It is calculated by using the cooling rate divided by the power consumption. A higher value of COP reflects a higher efficiency of a heat pump. In this paper, the COPs for both GSHP and the system are calculated using the following equations:

$$COP_{heat\ pump} = \frac{q_{cooling}}{P_{heat\ pump}} \tag{6}$$

$$COP_{system} = \frac{q_{cooling}}{P_{heat\ pump} + P_{water\ pumps}} \quad (7)$$

where

$q_{cooling}$ is the cooling rate of the heat pump (W),

$P_{heat\ pump}$ is the power input of the heat pump (W),

$P_{water\ pump}$ is the total power consumption of the water pumps in the system (W).

3.3 Modeling with Modelica

A Modelica –based dynamic model is used to study the behaviors of the solar powered GSHP system. The simulated results from the Modelica model will be compared with measurements from the on-site sensors. The component models are directly from the Modelica libraries, and the initial conditions were modified based on the actual conditions and system's manufacture specification. Figure 3-6 shows a parameter dialog box of the initial conditions. The working fluid in the studied GSHP is R410a and the secondary side fluid is water at the condenser side and air at the evaporator side.

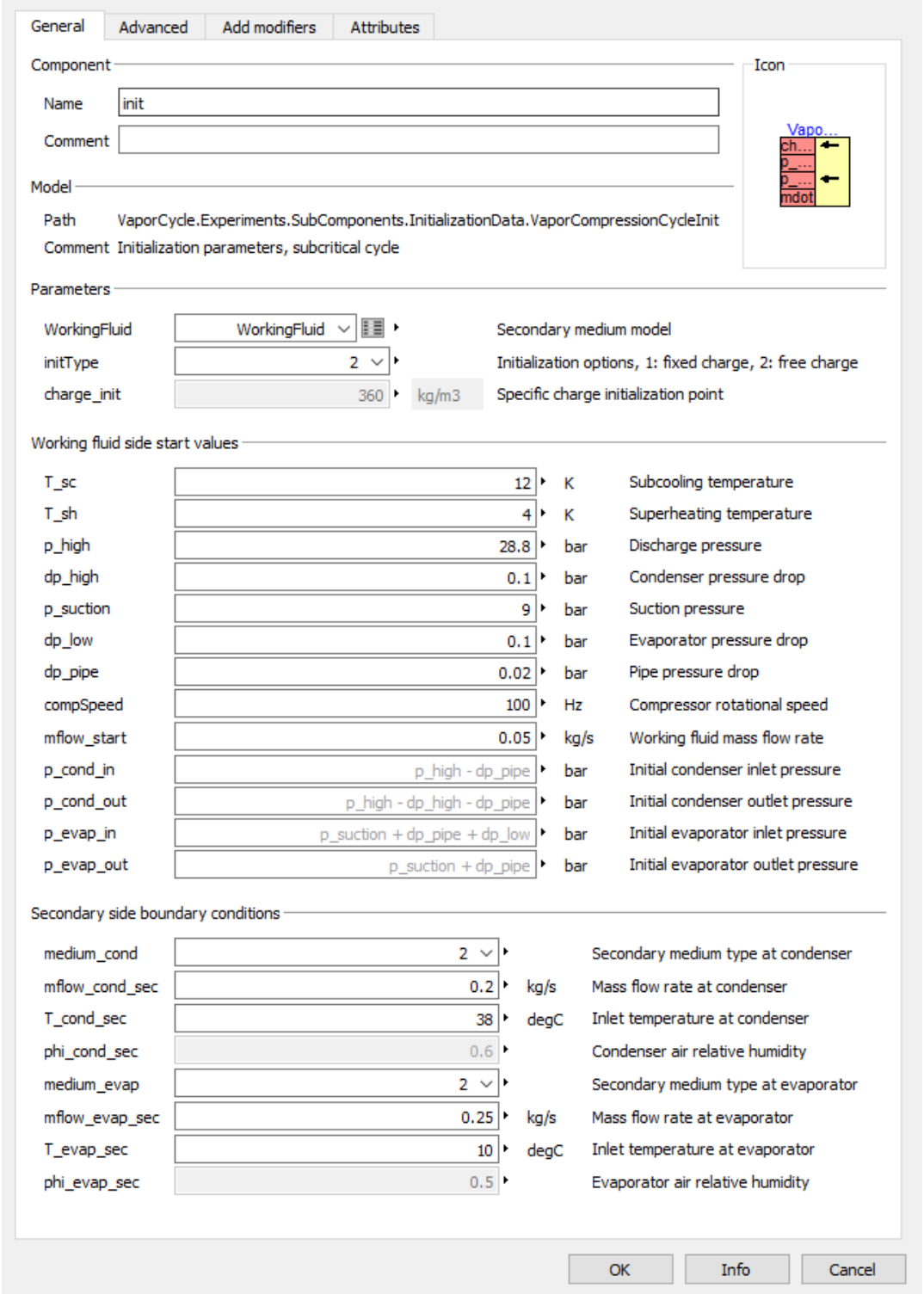

Figure 3-6 Initial Condition Dialog Box.

The current Modelica model is a water-to-water heat pump with working fluid R410a. Figure 3-7 shows the overall structure of the model. R410a has a relative higher working pressure, at condensing temperature of 120 degree Celsius, the high side pressure is 418 psig, and at 45 degree Celsius evaporator saturation temperature, the lower side pressure is 130 psig [23]. Meanwhile, some other initial values were set up using data from the actual GSHP model. Table 3-7 shows the initial conditions used for this simulation.

Currently, the two wells are treated as a heat source and a heat sink with constant temperatures. In the near future, a Modelcia-based well heat exchanger model will be developed.

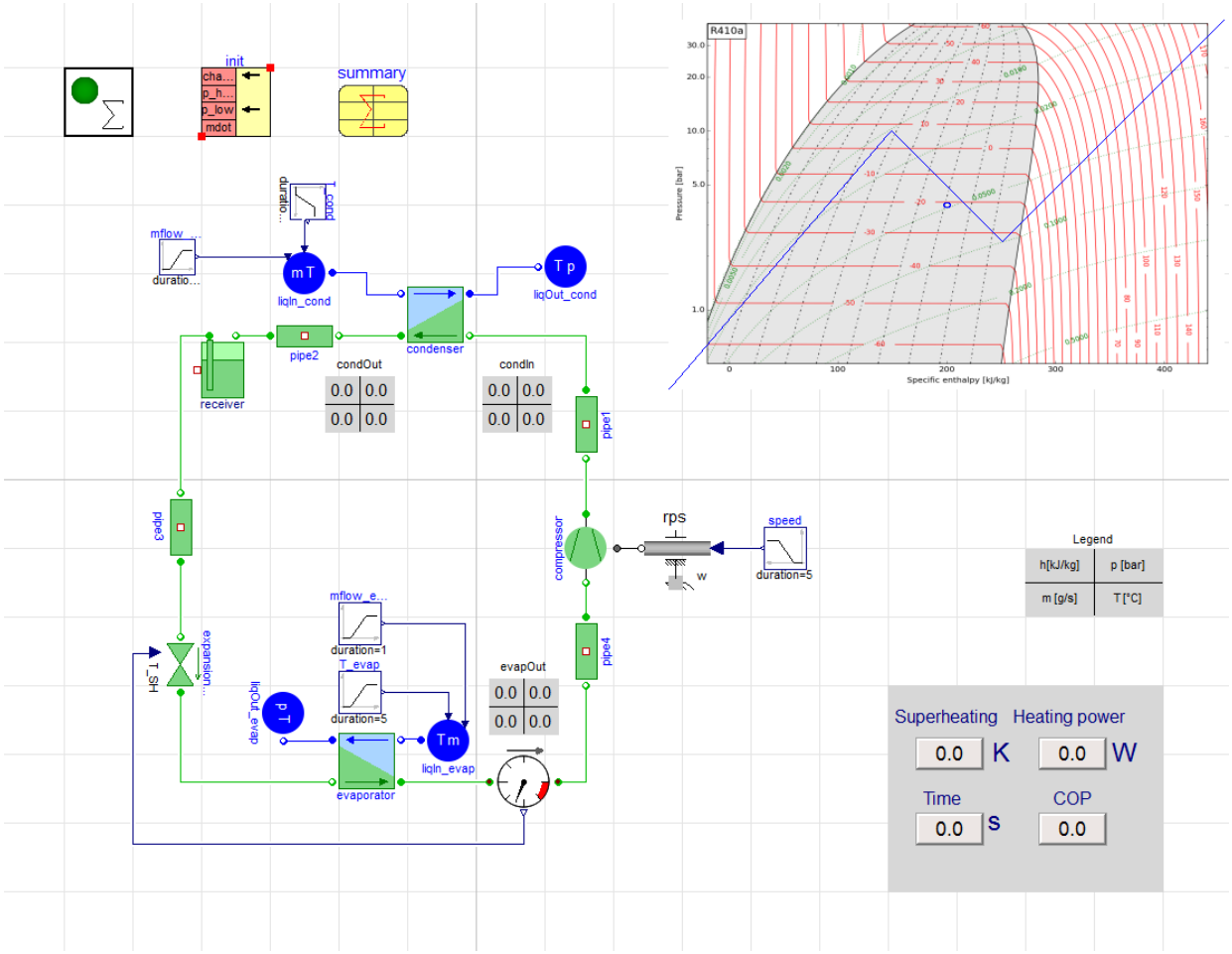

Figure 3-7 Overall Structure of a Heat Pump.

Table 3-7 Initial Condition Value.

Event	Unit	Value
Discharge Pressure	bar	28.8
Suction Pressure	bar	9
Compressor Speed	Hz	100
Condenser Inlet Temperature	Celsius	38
Evaporator Inlet Temperature	Celsius	10
Mass Flow Rate at Condenser	kg/s	0.2
Mass Flow Rate at Evaporator	kg/s	0.25

3.4 Simulation

To simulate the Modelica model in Dymola is simple. In general, it is better to get a relatively longer simulation time since the system takes some time to reach the steady state. In this case, the simulation time is set as from 0 to 1500 seconds. Figure 3-8 shows an example of the simulation setup dialog box. The solver chosen for this simulation is Dassl, which is a default solver for a differential/algebraic system.

After the simulation is done, the output variable of the model will be listed on the left-hand side of the window, and the plot of the variable can be shown on the other side.

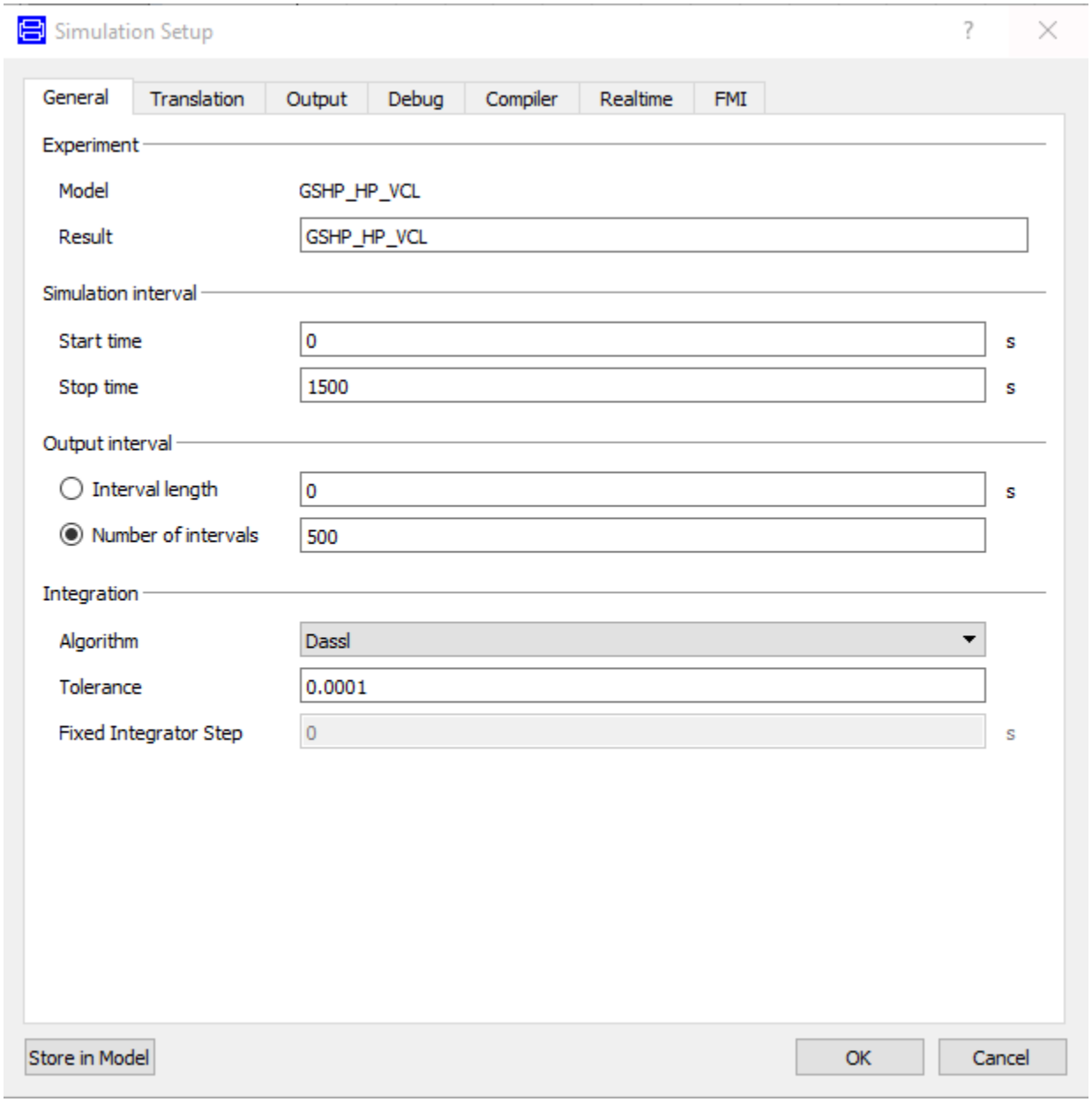

Figure 3-8 Simulation Setup Dialog Box.

4. RESULTS AND DISCUSSIONS

4.1 Measured Results

4.1.1 Solar Energy Collection/Power Generation

In this paper, a four-week long data between January 30th, 2016 to February 27th, 2016 was collected and analyzed. Figure 4-1 shows the solar energy collection/power generation results over the time in February. The area under the curve represents the collection of solar energy, high wave crest means relatively high solar power generation (W) and vice versa. In addition, the fluctuation of the curve reflects the change of the available solar irradiance. According to the plot, for some days, such as February 8th and 9th, the highest charging power during the experiment period was around 750 Watts. Meanwhile, for some days, such as February 15th and 22nd, the weather could be the possible reason for a lower peak charging power of around 100 Watts.

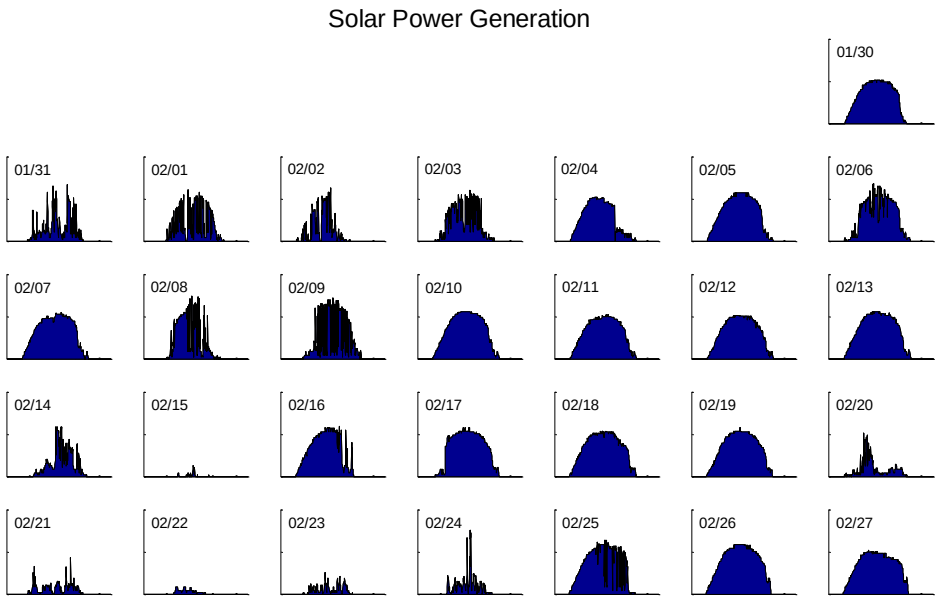

Figure 4-1 Solar Energy Collection (in Watts) Over the Time in February 2016.

In addition, a further analysis was conducted between the theoretical power generation and actual power generation (as shown in Figure 4-2), the red solid line represents the theoretical power generation from the solar panels, and the blue dot-dash line represents the actual values based on measurements using Equation (1). The theoretical results were calculated using solar radiation heat flux from the on-site weather station and manufacturer's specification [24] of the solar panels. According to the specification, when the cell temperature is 25.0˚C and the solar irradiance is at 1000 W/m^2 level, the power generation is 50 Watts for each panel. In this test, 16 panels were used to charge the batteries. This means an 800 Watts charging power in total.

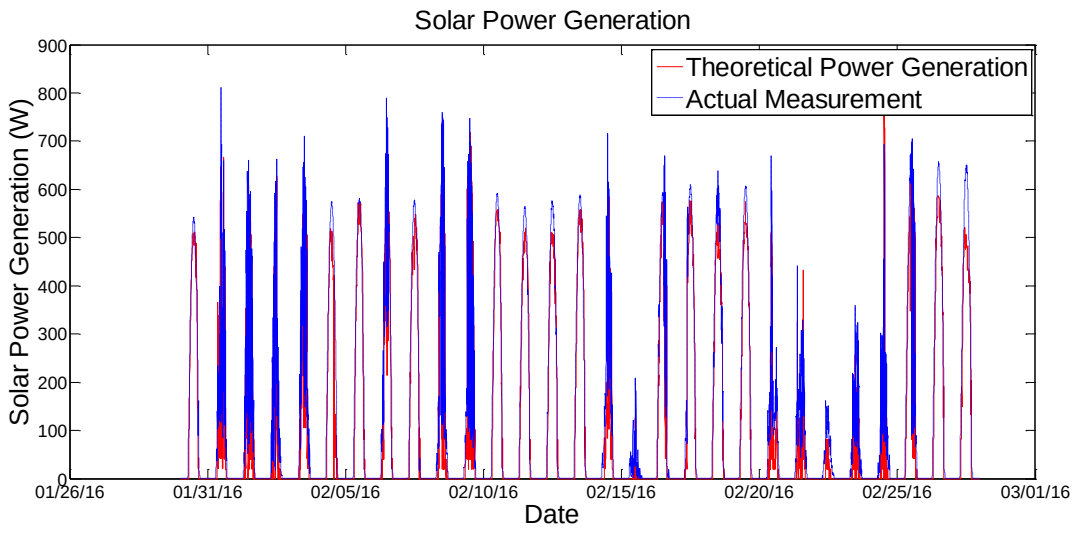

Figure 4-2 Comparison Between the Theoretical and Actual Power Generation from the Solar Panels.

The further analysis shows that the theoretical generated energy was about 297 MJ, while the actual measured generated energy from the solar panels was 242 MJ. The percentage difference between the theoretical value and actual measurement was about 18.6%. There are several reasons that could contribute such difference:

1. The actual location of the on-site weather station is higher than those solar panels, which means a solar panel at the location of the weather station can collect more solar radiation compared with the actual solar panels.
2. The actual charging rate depends on the state of charge (SOC) of the batteries. Full charging power was applied only when the SOC was relative low, and with the increase of the SOC, the charging rate could be reduced, which caused the sensors detect a low charging power. Meanwhile, the theoretical result is based on the on-site weather station, and the applied algorithm assumed the batteries were charged with full power. Therefore, the actual

charged energy could be less than the theoretical value at the time when SOC was relatively higher.

3. Some of solar panels were installed about 20 years ago, the degradation on the performance could be another factor that may cause the actual reading is less than the theoretical result.

4.1.2 Charge and Discharge

There is a need to know the charge and discharge time of the batteries. Calculations of the charge and discharge time were based on the assumptions listed in section 3.2.5.

From the measured data, the peak power generation from the solar panels was about 754 Watts. If all the batteries were empty and the electricity generation from the solar panel was assumed to be at the peak value always, it would take 12.7 hours for the batteries to be fully charged by using Equation (2). At the same time, the test also showed that the heat pump energy consumption was about 600 Watts during the operation, which means the batteries could be drained in about 9.5 hours if the heat pump kept running by only using power provided by the batteries. The experiment was conducted in February with a relatively short daylight time and a low solar radiation level. If the same test was done in the summer, the peak solar radiation flux and the solar panel power generation would be higher than the current result, which leads to a higher charging power and a less charging time. Figure 4-3 shows the solar radiation flux through the year of 2015, and there was about 25% more solar radiation in the summer than in February. By combining the monthly plots together, it is easy to tell that the solar radiation peak appeared between May to September of the year (as shown in Figure 4-4).

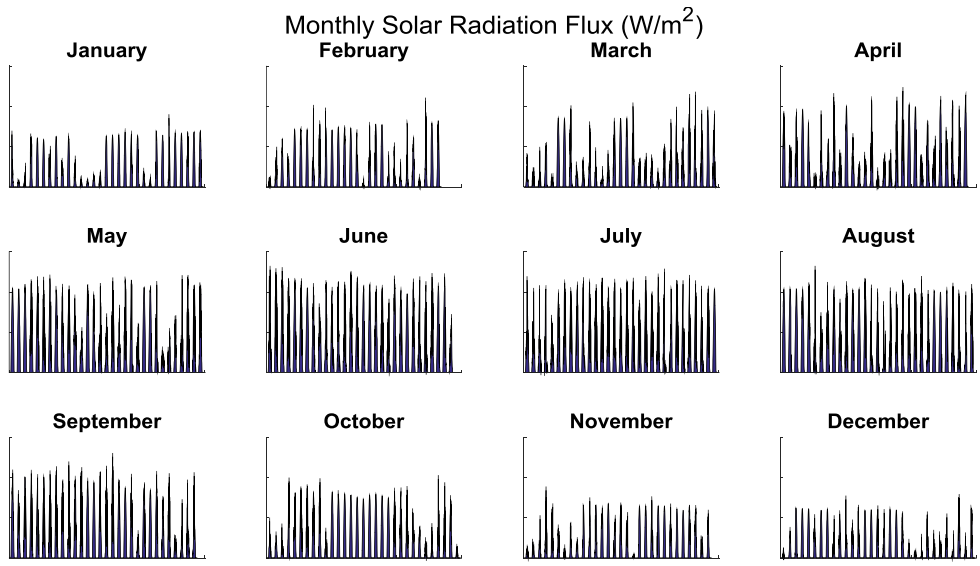

Figure 4-3 Monthly Plots of Solar Radiation Flux (W/m^2).

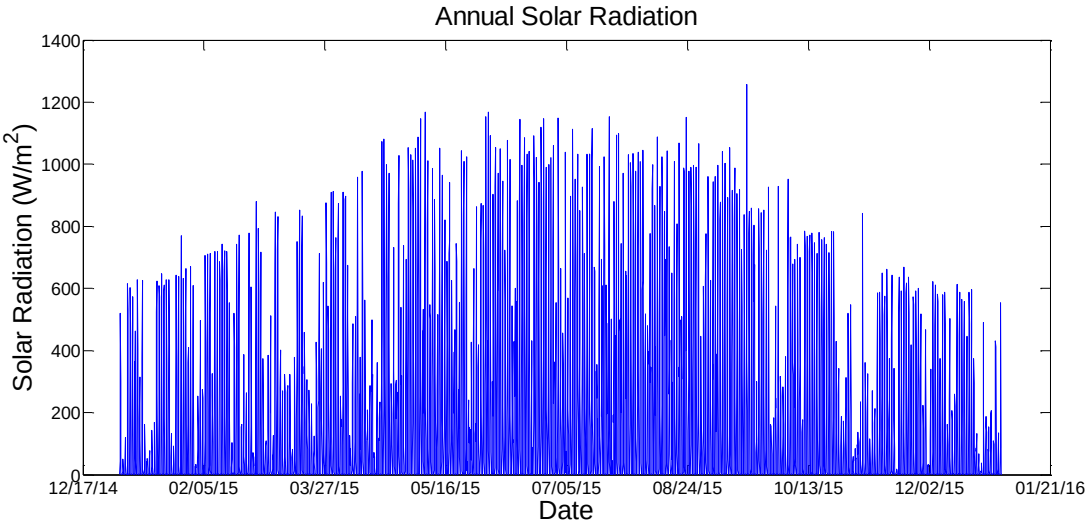

Figure 4-4 Annual Solar Radiation Flux (W/m^2).

4.1.3 Heat Pump Energy Balance

In the cooling mode, the energy balance of the heat pump was maintained among the electric power consumption, rejected energy and cooling rate. Since the heat pump power

consumption was constant during the test, and the heat rejection from the air-side to the water-side could be calculated by using measured temperatures and flow rate data. The cooling rate of the heat pump was calculated to be 1,938 Watts using Equation (5). However, the manufacturer specified the rated cooling rate of this heat pump is 2,638 Watts. The actual cooling rate is 73.5% of the rated value. This difference might cause by the fact that the rated value was tested in the lab at the standard rating condition. According to the standard rating condition under a cooling mode [3], the air temperatures entering indoor portion of unit are 26.7˚C (80˚F) dry-bulb and 19.4˚C (67˚F) wet-bulb. Dry-bulb air temperatures surrounding the unit are 26.7˚C (80˚F). Refrigerant temperatures from the test water coil (liquid line) are 25.0˚C (77˚F). However, for the actual operation in this study, all these conditions are different. It is not surprised there are variations in the testing result since the test was accomplished at a different environment.

The COP was calculated using the actual cooling rate from the total energy balance calculation, and the power consumption from the actual measurement. In the standard rating condition, the COP of the tested heat pump was 3.8 listed in the manufacturer catalog. By using Equation (6), the average COP of the heat pump was 3.23 during the test period. For the system COP, more components need to be considered, which means the value of COP would be decreased comparing with the COP of the heat pump itself only. In this test, the average COP of the system was 2.67 by using Equation (7).

4.2 Modeling Results

Using a Modelcia-based dynamic model, the GSHP system's behaviors can be presented and visualized easily. Since the model is still under development, no comparisons with

measurement will be presented at this moment. As Figure 4-5 shows, the COP of the system maintains around 2.9 when the system goes into a steady state.

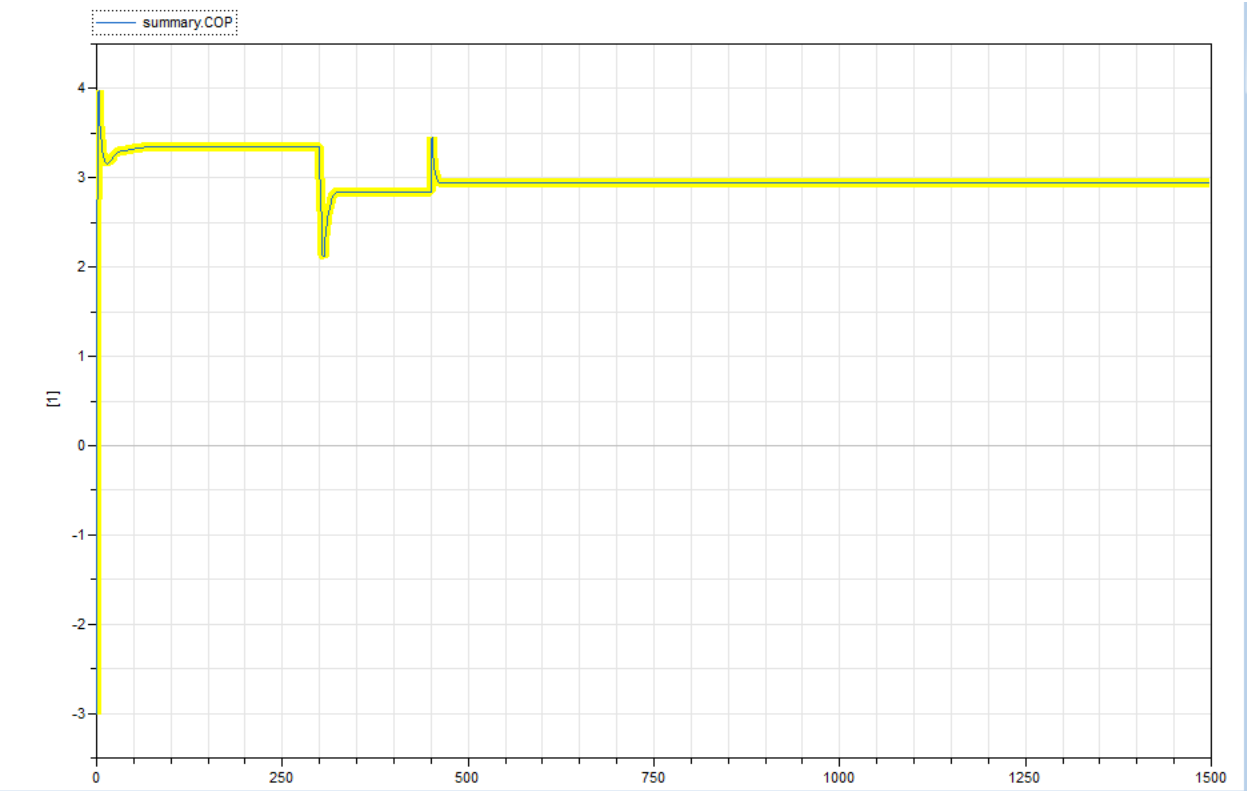

Figure 4-5 Simulation Result (COP).

5. FUTURE WORK

Some future works are listed as follows:

5.1 Test Rig Improvement

- The capacity of the battery banks will be extended, a larger battery capacity will offer relatively longer operating time. In addition, some synchronizing relays will be added which will help better control the well pump and the circulation water pump. Currently, both the well pump and the water pump were kept running during the test. The proposed synchronizing relays help control the running time of the water pump and well pump, the pumps would work only when the heat pump is on demand.
- The air flow meter will be added to measure the air flow rate, which allows to measure the cooling rate more accurately.

5.2 Model Development, and Validation

Due to some limitations, the Modelica model presented in this thesis is a water-to-water heat pump system instead of a water-to-air heat pump system used in the test rig. Further investigations and modifications will be conducted to model the actual water-to-air GSHP system. Well ground heat exchanger model in Modelica will be developed as well. In addition, the solar panel system will be modeled and integrated with the GSHP system.

A comprehensive system model of solar powered ground source heat pump system will be validated using measurement from the test rig. Testing data will be collected for a longer period for both heating and cooling modes.

5.3 Model Applications

After the system model is developed and validated, this dynamic model will be used for the following applications:

- Model-based control of the solar power generation system and ground source heat pump system, and the combination of these systems for a better building and grid integration.
- Local heat pump controller design using this dynamic model in the Hardware-in-the-loop testing.

REFERENCES

1. https://www.modelica.org/.
2. Berardi, U., Building energy consumption in US, EU, and BRIC countries. Procedia Engineering, 2015. 118: p. 128-136.
3. Qian, D., et al., Investigation on A Ground Source Heat Pump System Integrated With Renewable Sources. 2016.
4. Energy, U., Buildings Energy Data Book, in, 2012. 2011.
5. Chamoun, M., et al., Dynamic model of an industrial heat pump using water as refrigerant. international journal of refrigeration, 2012. 35(4): p. 1080-1091.
6. Shen, P. and N. Lior, Vulnerability to climate change impacts of present renewable energy systems designed for achieving net-zero energy buildings. Energy, 2016. 114: p. 1288-1305.
7. Balta, M.T., I. Dincer, and A. Hepbasli, Potential methods for geothermal-based hydrogen production. international journal of hydrogen energy, 2010. 35(10): p. 4949-4961.
8. Ozgener, O. and A. Hepbasli, A review on the energy and exergy analysis of solar assisted heat pump systems. Renewable and Sustainable Energy Reviews, 2007. 11(3): p. 482-496.
9. Hepbasli, A., Exergetic modeling and assessment of solar assisted domestic hot water tank integrated ground-source heat pump systems for residences. Energy and Buildings, 2007. 39(12): p. 1211-1217.
10. Huttrer, G.W., Geothermal heat pumps: An increasingly successful technology. Renewable Energy, 1997. 10(2-3): p. 481-488.
11. Self, S.J., B.V. Reddy, and M.A. Rosen, Geothermal heat pump systems: Status review and comparison with other heating options. Applied Energy, 2013. 101: p. 341-348.
12. Zhu, Y., Y. Tao, and R. Rayegan, A comparison of deterministic and probabilistic life cycle cost analyses of ground source heat pump (GSHP) applications in hot and humid climate. Energy and Buildings, 2012. 55: p. 312-321.
13. Shonder, J.A., et al., Geothermal heat pumps in K-12 schools: A case study of the Lincoln, Nebraska schools. US Department of Energy Publications, 2000: p. 30.

14. Chiasson, A., Life-cycle cost study of a geothermal heat pump system. Geo-Heat Center, Oregon Institute of Technology, Klamath Falls, OR, 2006.

15. Kannan, N. and D. Vakeesan, Solar energy for future world:-A review. Renewable and Sustainable Energy Reviews, 2016. 62: p. 1092-1105.

16. Tripathy, M., P. Sadhu, and S. Panda, A critical review on building integrated photovoltaic products and their applications. Renewable and Sustainable Energy Reviews, 2016. 61: p. 451-465.

17. Ortega-Izquierdo, M. and P. del Río, Benefits and costs of renewable electricity in Europe. Renewable and Sustainable Energy Reviews, 2016. 61: p. 372-383.

18. Mattsson, S.E., H. Elmqvist, and M. Otter, Physical system modeling with Modelica. Control Engineering Practice, 1998. 6(4): p. 501-510.

19. Mortada, S., et al., Dynamic modeling of an integrated air-to-air heat pump using Modelica. international journal of refrigeration, 2012. 35(5): p. 1335-1348.

20. Assaf, K., A. Zoughaib, and D. Clodic, Modelica-based modelling and simulation of dry-expansion shell-and-tube evaporators working with alternative refrigerant mixtures. International Journal of Refrigeration, 2011. 34(6): p. 1471-1482.

21. http://www.modelon.com/products/modelica-libraries/vapor-cycle-library/.

22. Tummescheit, H., J. Eborn, and K. Prölss. Airconditioning–a Modelica library for dynamic simulation of AC systems. in Paper presented at the 4th International Modelica Conference. 2005.

23. Adelekan, D., et al., Exergy, Performance And Environmental Impact Analysis Of Compression Refrigeration Systems. 2014.

24. http://www.siemen.co.uk/sm50_h.html.